Appendix 4: Sensitivity analysis

4.1. Model results including an evaporite end-member

Model results when including an evaporite end-member show similar trends as our primary inversion model (Fig. S15). In this inversion the evaporite end member has $Ca^{2+}/\Sigma^{+} = 0.45\pm0.18$, $Mg^{2+}/\Sigma^{+} = 0.09\pm0.06$, $Na^{+}/\Sigma^{+} = 0.45\pm0.16$, $K^{+}/\Sigma^{+}=0\pm0$, $SO_4^{2-}/\Sigma^{+} = 0.34\pm0.23$, $Cl^{-}/\Sigma^{+} = 0.44\pm0.18$. However, as in Torres et al. (2017), we force set the chemical composition of the evaporite end-member to reflect a stoichiometry of $CaSO_4$ and HCl. As a result, the values of SO_4^{2-}/Σ^{+} and Cl^{-}/Σ^{+} are not pulled from the indicated distributions, but rather are set to equal the sum of Ca^{2+}/Σ^{+} and Mg^{2+}/Σ^{+} or Na^{+}/Σ^{+}, respectively. Rather than assigning values of $Cl_{Critical}$, the inversion apportions the Cl^{-} budget between precipitation and the evaporite end-member.

4.2. Model results including a hot spring end-member

In this simulation (Fig. S16), the hot spring end member has $Ca^{2+}/\Sigma^{+} = 0.17\pm0.12$, $Mg^{2+}/\Sigma^{+} = 0.09\pm0.11$, $Na^{+}/\Sigma^{+} = 0.69\pm0.25$, $K^{+}/\Sigma^{+}=0.06\pm0.03$, $SO_4^{2-}/\Sigma^{+} = 0.06\pm0.02$, $Cl^{-}/\Sigma^{+} = 0.02\pm0.04$. Rather than assigning values of $Cl_{Critical}$, the inversion apportions the Cl^{-} budget between precipitation and the spring end-member. Because the spring has very high Na^{+}/Cl^{-}, a small apportionment of the Cl^{-} budget to springs explains a significant fraction of the Na^{+} budget. As a result, inclusion of a hot spring increases the fraction of carbonate weathering (R).

4.3. Model results without [K^{+}] or [Cl^{-}] in the inversion

Pre-collection acid washing is a potential source of Na^{+}, K^{+}, and Cl^{-} contamination. While [Na^{+}] exhibits a monsoon decline seen in prior data, [K^{+}] and [Cl^{-}] do not decline coherently with increases in discharge. We argue in the main text that this observation is a robust feature of the data related to dynamics of glacial weathering (Anderson et al., 1997, 2000) or landslides (Emberson et al., 2017), but it is also possibly indicative of a procedural blank. When only [Ca^{2+}], [Mg^{2+}], [Na^{+}], and [SO_4^{2-}] are inverted without [K^{+}] or [Cl^{-}], we recover monsoon increases in the fraction of carbonate weathering consistent with prior studies (Fig. S17, Tipper et al., 2006).

4.4. Forward model of carbonate and silicate contributions

Prior research has used a forward-model to calculate the fractional contributions of carbonate and silicate rocks (Galy & France-Lanord, 1999). The outline of this calculation is to (1) remove [Cl^{-}] from observations, (2) attribute a fraction of the remaining [Ca^{2+}] and [Mg^{2+}] to silicate weathering and the residual to carbonate weathering, and (3) calculate the flux of carbonate and silicate alkalinity. Below we show that the results of this calculation are extremely similar to those of our full inversion model (Fig. S18).

(1) Assume all Cl^{-} derives from seawater (eq. S1), either through weathering of evaporites or direct input through precipitation. For this correction we use the seawater chemistry of Sarmiento & Gruber (2006). In eq. S1, the variable Z stands for any dissolved ion concentration, and concentrations corrected for Cl^{-} are indicated with a superscripted *.

$$[Z_i]^*_{riv} = [Z_i]_{riv} - [Cl^-]_{riv}\left(\frac{[Z_i]_{seawater}}{[Cl^-]_{seawater}}\right) \qquad \text{(eq. S1)}$$

(2) Assume all remaining Na^{+} and K^{+} derive from silicate weathering (eqs. S2, S3). For Ca^{2+} and Mg^{2+}, scale by the Ca^{2+}/Na^{+} ($X^{slct}_{Ca^{2+}/Na^{+}}$) and Mg^{2+}/K^{+} ratios ($X^{slct}_{Mg^{2+}/K^{+}}$) of silicate rocks (eqs. S4-S7). We take $X^{slct}_{Ca^{2+}/Na^{+}}$=0.2±0.1 and $X^{slct}_{Mg^{2+}/K^{+}}$=0.5±0.2 (Galy & France-Lanord, 1999).

$[Na]_{silicate} = [Na]^*$ (eq. S2)

$[K]_{silicate} = [K]^*$ (eq. S3)

$[Ca]_{sililcate} = [Na]^* * X^{slct}_{Ca^{2+}/Na^+}$ (eq. S4)

$[Mg]_{silicate} = [K]^* * X^{slct}_{Mg^{2+}/K^+}$ (eq. S5)

$[Ca]_{carbonate} = [Ca]^* - [Ca]_{silicate}$ (eq. S6)

$[Mg]_{carbonate} = [Mg]^* - [Mg]_{silicate}$ (eq. S7)

(3) Calculate R as the fraction of Cl-corrected cations derived from carbonate weathering (eq. S8). Calculate Z by assuming that 100% of $[SO_4^{2-}]^*$ is sourced from FeS_2 oxidation (eq. S9).

$$R = \frac{2[Ca^{2+}]_{carbonate}+2[Mg^{2+}]_{carbonate}}{2[Ca^{2+}]^*+2[Mg^{2+}]^*+[Na^+]^*+[K^+]^*} \quad \text{(eq. S8)}$$

$$Z = \frac{2[SO_4^{2-}]^*}{2[Ca^{2+}]^*+2[Mg^{2+}]^*+[Na^+]^*+[K^+]^*} \quad \text{(eq. S9)}$$

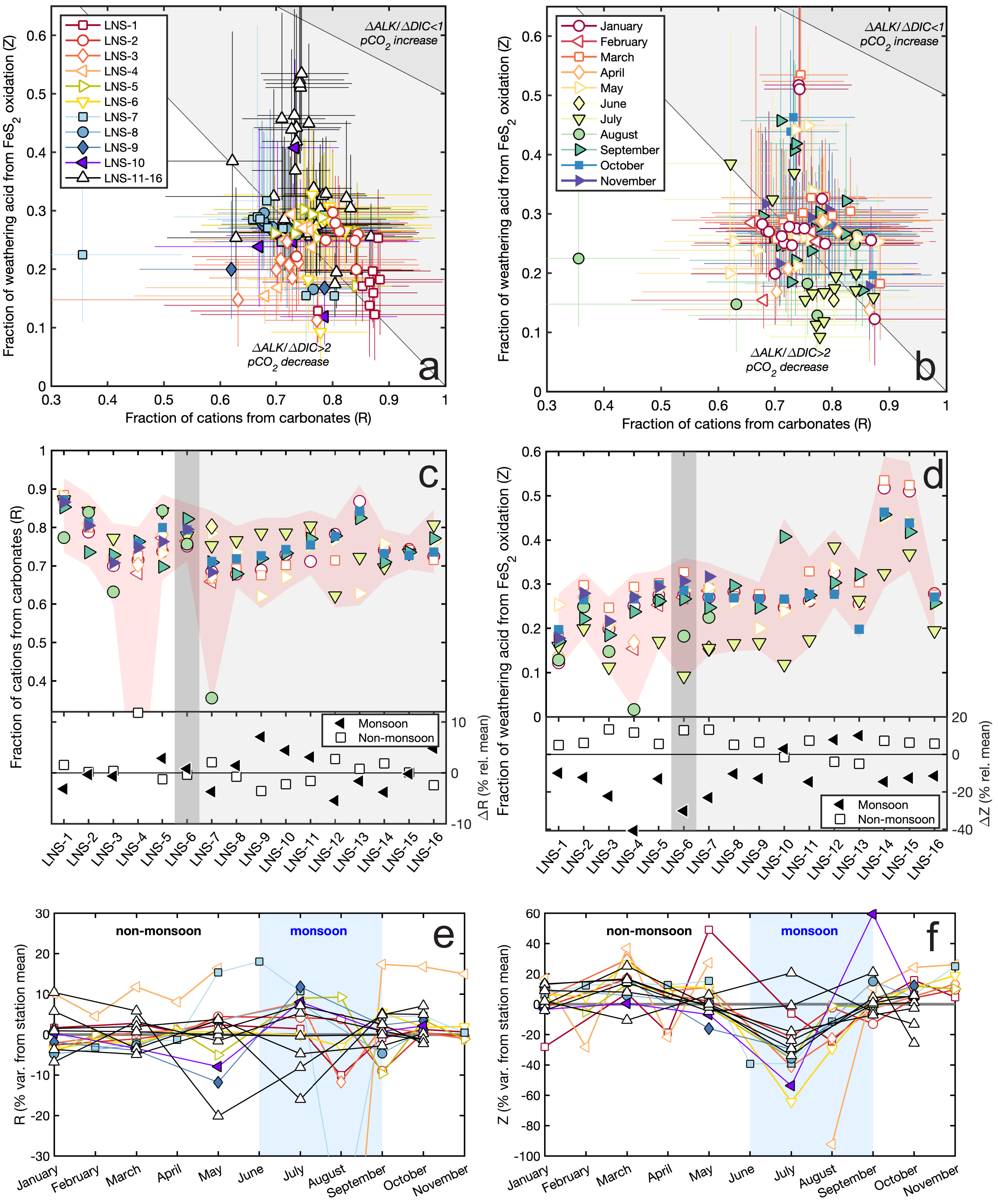

Fig. S15: Fraction of weathering acid from FeS$_2$ oxidation (Z) against the fraction of cations from carbonate weathering (R) when the inversion includes an evaporite, color-coded by either (a) site of sample collection or (b) month of sample collection. (c, d) R and Z against sample location. (e, f) Timeseries of R and Z.

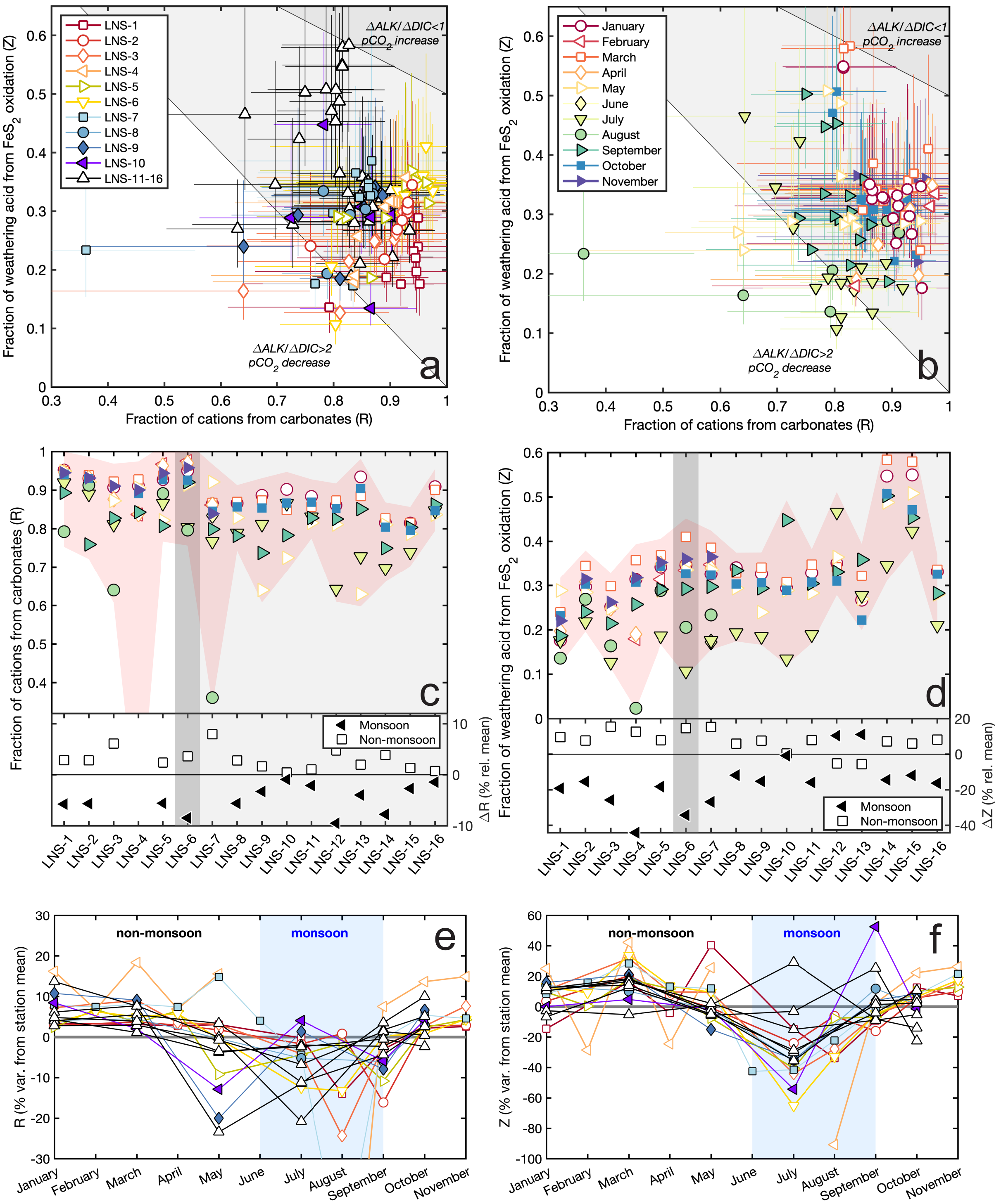

Fig. S16: Fraction of weathering acid from FeS$_2$ oxidation (Z) against the fraction of cations from carbonate weathering (R) when the inversion includes a hot spring, color-coded by either (a) site of sample collection or (b) month of sample collection. (c, d) R and Z against sample location. (e, f) Timeseries of R and Z.

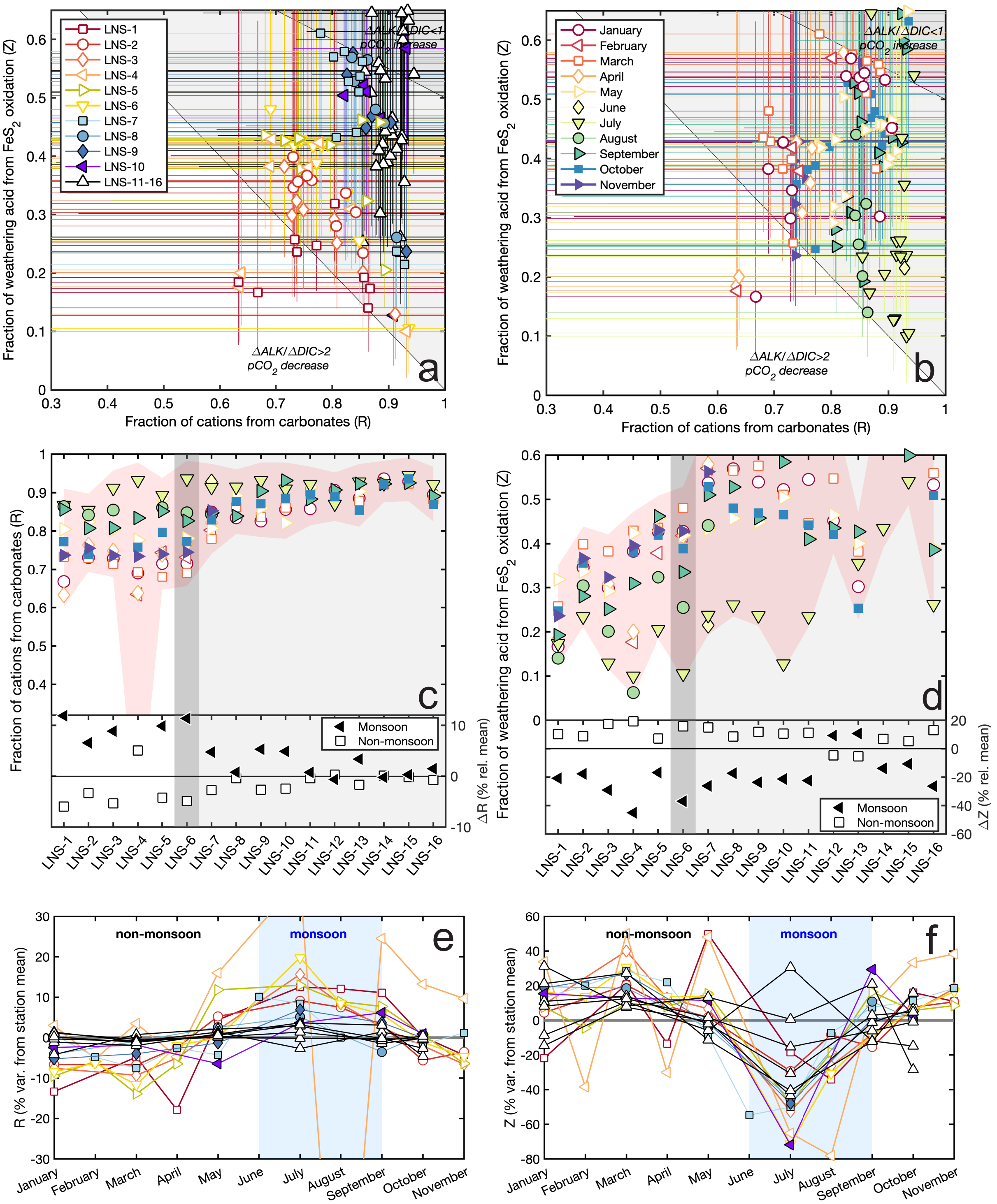

Fig. S17: Fraction of weathering acid from FeS_2 oxidation (Z) against the fraction of cations from carbonate weathering (R) when the inversion does not include K^+ or Cl^-, color-coded by either (a) site of sample collection or (b) month of sample collection. Note the extreme range of successful simulation results. (c, d) R and Z against sample location. (e, f) Timeseries of R and Z. These results show a monsoon increase in R consistent with prior studies (Tipper et al., 2006).

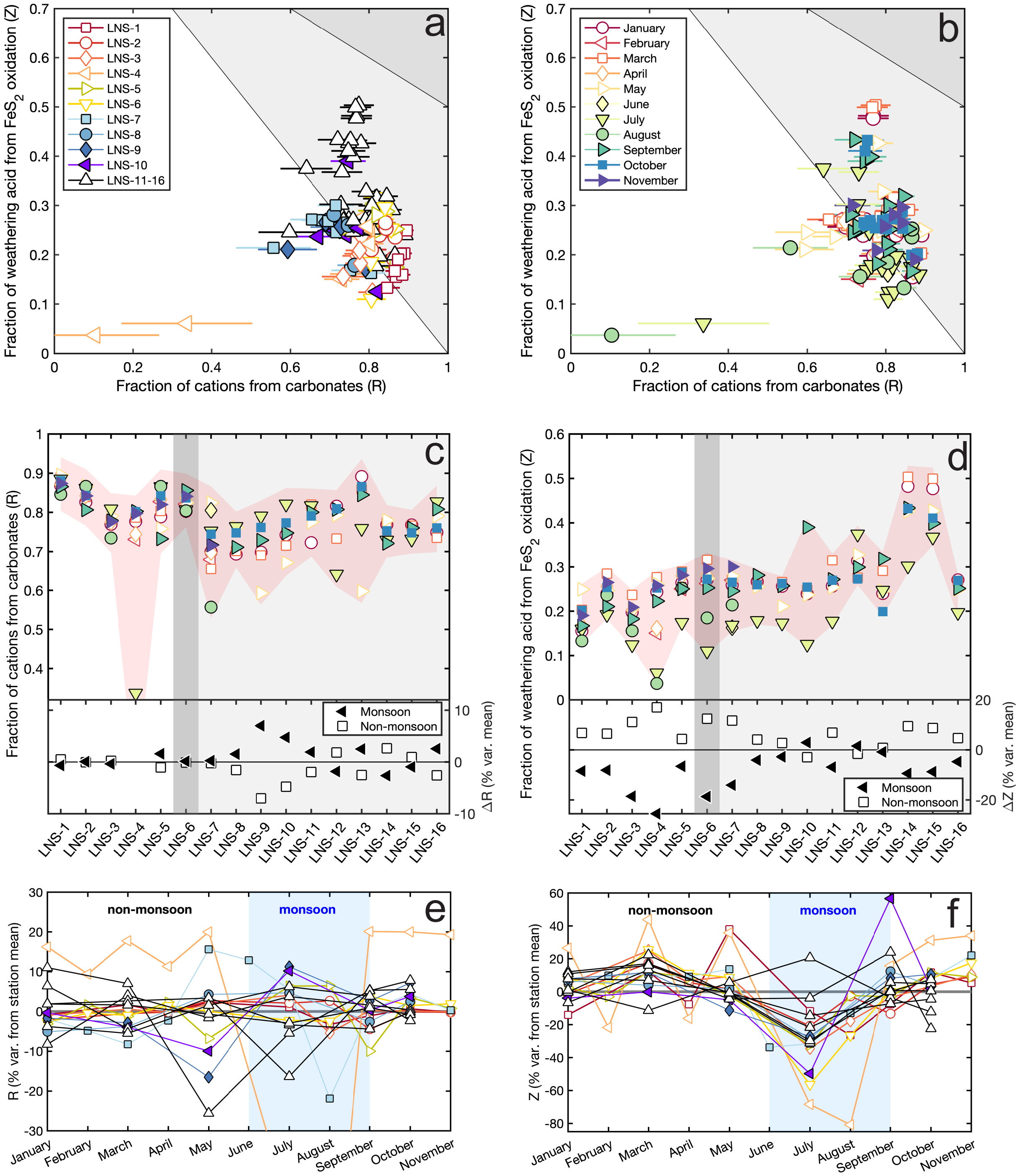

Fig. S18: Fraction of weathering acid from FeS_2 oxidation (Z) against the fraction of cations from carbonate weathering (R) calculated using a forward model, color-coded by either (a) site of sample collection or (b) month of sample collection. (c) R against sample location and (d) Z against sampling location. (e, f) Timeseries of R and Z. Results are very similar to those reached using the full inversion model discussed in the text (Fig. 9).

Appendix 5: References

Andermann C., Bonnet S., & Gloaguen R. (2011). Evaluation of precipitation data sets along the Himalayan front. *Geochemistry, Geophysics, Geosystems*, **12(7)**.

Anderson S., Drever J. I., & Humphrey N. F. (1997). Chemical weathering in glacial environments. *Geology*, **25(5)**, 399-402.

Anderson S. P., Drever J. I., Frost C. D., & Holden P. (2000). Chemical weathering in the foreland of a retreating glacier. *Geochimica et Cosmochimica Acta*, **64(7)**, 1173-1189.

Balestrini R., Polesello S., & Sacchi E. (2014). Chemistry and isotopic composition of precipitation and surface waters in Khumbu valley (Nepal Himalaya): N dynamics of high elevation basins. *Science of the Total Environment*, **485**, 681-692.

Becker J. A., Bickle M. J., Galy A., & Holland T. J. (2008). Himalayan metamorphic CO_2 fluxes: Quantitative constraints from hydrothermal springs. *Earth and Planetary Science Letters,* **265(3-4)**, 616-629.

Berner R. A. (1971). Worldwide sulfur pollution of rivers. *Journal of Geophysical Research*, **76(27)**, 6597-6600.

Bhatt M. P., Masuzawa T., Yamamoto M., Sakai A., & Fujita K. (2000). Seasonal changes in dissolved chemical composition and flux of meltwater draining from Lirung Glacier in the Nepal Himalayas. *IAHS Publication* **264**, 277-288.

Bhatt M. P., Masuzawa T., Yamamoto M., & Gardner K. H. (2009). Spatial variations in chemical compositions along Langtang–Narayani river system in central Nepal. *Environmental geology*, **57(3)**, 557-569.

Bhatt M. P., Hartmann J., & Acevedo M. F. (2018). Seasonal variations of biogeochemical matter export along the Langtang-Narayani river system in central Himalaya. *Geochimica et Cosmochimica Acta*, **238**, 208-234.

Bickle M. J., Chapman H. J., Bunbury J., Harris N. B., Fairchild I. J., Ahmad T., & Pomiès C. (2005). Relative contributions of silicate and carbonate rocks to riverine Sr fluxes in the headwaters of the Ganges. *Geochimica et Cosmochimica Acta*, **69(9)**, 2221-2240.

Bickle M. J., Tipper E. D., Galy A., Chapman H., & Harris N. (2015). On discrimination between carbonate and silicate inputs to Himalayan rivers. *American Journal of Science*, **315(2)**, 120-166.

Bordet P., Colchen M., Krummenacher D., Lefort P., Mouterde R., Remy M., 1971. Recherches Geologiques dans l'Himalaya du Nepal region de la Thakkhola. *Editions du centre national de la recherche scientifique*.

Burke A., Present T. M., Paris G., Rae E. C., Sandilands B. H., Gaillardet J., ... & Voss B. M. (2018). Sulfur isotopes in rivers: Insights into global weathering budgets, pyrite oxidation, and the modern sulfur cycle. *Earth and Planetary Science Letters*, **496**, 168-177.

Claypool G. E., Holser W. T., Kaplan I. R., Sakai H., & Zak I. (1980). The age curves of sulfur and oxygen isotopes in marine sulfate and their mutual interpretation. *Chemical Geology*, **28**, 199-260.

Collins R., & Jenkins A. (1996). The impact of agricultural land use on stream chemistry in the Middle Hills of the Himalayas, Nepal. *Journal of Hydrology*, **185(1-4)**, 71-86.

Dalai T. K., Krishnaswami S., & Sarin M. M. (2002). Major ion chemistry in the headwaters of the Yamuna river system: Chemical weathering, its temperature dependence and CO_2 consumption in the Himalaya. *Geochimica et Cosmochimica Acta*, **66(19)**, 3397-3416.

Emberson R., Galy A., & Hovius N. (2017). Combined effect of carbonate and biotite dissolution in landslides biases silicate weathering proxies. *Geochimica et Cosmochimica Acta*, **213**, 418-434.

Evans M. J., Derry L. A., Anderson S. P., & France-Lanord C. (2001). Hydrothermal source of radiogenic Sr to Himalayan rivers. *Geology*, **29(9)**, 803-806.

Evans M. J., Derry L. A., & France-Lanord C. (2004). Geothermal fluxes of alkalinity in the Narayani river system of central Nepal. *Geochemistry, Geophysics, Geosystems*, **5(8)**.

Evans M. J., Derry L. A., & France-Lanord C. (2008). Degassing of metamorphic carbon dioxide from the Nepal Himalaya. *Geochemistry, Geophysics, Geosystems*, **9(4)**.

Fort M. (1996). Late Cenozoic environmental changes and uplift on the northern side of the central Himalaya: a reappraisal from field data. *Palaeogeography, Palaeoclimatology, Palaeoecology*, **120(1-2)**, 123-145.

France-Lanord C., & Derry L. A. (1997). Organic carbon burial forcing of the carbon cycle from Himalayan erosion. *Nature*, **390(6655)**, 65.

Gaillardet J., Dupré B., Louvat P., & Allegre C. J. (1999). Global silicate weathering and CO_2 consumption rates deduced from the chemistry of large rivers. *Chemical geology*, **159(1-4)**, 3-30.

Galy A., & France-Lanord C. (1999). Weathering processes in the Ganges–Brahmaputra basin and the riverine alkalinity budget. *Chemical Geology*, **159(1-4)**, 31-60.

Handa B.K. (1968). The chemical composition of rain water in some parts of North India. *Indian journal of meteorology & geophysics,* **19**, 175-180.

Harris N., Bickle M., Chapman H., Fairchild I., & Bunbury J. (1998). The significance of Himalayan rivers for silicate weathering rates: evidence from the Bhote Kosi tributary. *Chemical Geology*, **144(3-4)**, 205-220.

Hren M. T., Chamberlain C. P., Hilley G. E., Blisniuk P. M., & Bookhagen B. (2007). Major ion chemistry of the Yarlung Tsangpo–Brahmaputra river: chemical weathering, erosion, and CO_2 consumption in the southern Tibetan plateau and eastern syntaxis of the Himalaya. *Geochimica et Cosmochimica Acta*, **71(12)**, 2907-2935.

Jacobson A. D., Blum J. D., & Walter L. M. (2002). Reconciling the elemental and Sr isotope composition of Himalayan weathering fluxes: insights from the carbonate geochemistry of stream waters. *Geochimica et Cosmochimica Acta*, ***66*****(19)**, 3417-3429.

Krishnaswami S., & Singh S. K. (1998). Silicate and carbonate weathering in the drainage basins of the Ganga-Ghaghara-Indus head waters: Contributions to major ion and Sr isotope geochemistry. *Proceedings of the Indian Academy of Sciences-Earth and Planetary Sciences*, **107(4)**, 283-291.

Krishnaswami S., Singh S. K., and Dalai T. K. (1999) Silicate weathering in the Himalaya: Role in contributing to major ions and radiogenic Sr to the Bay of Bengal. In Ocean Science, Trends and Future Directions (ed. B. L. K. Somayajulu), pp. 23–51. India.

Négrel P., Allègre C. J., Dupré B., & Lewin E. (1993). Erosion sources determined by inversion of major and trace element ratios and strontium isotopic ratios in river water: the Congo Basin case. *Earth and Planetary Science Letters*, **120(1-2)**, 59-76.

Pant R. R., Zhang F., Rehman F. U., Wang G., Ye, M., Zeng C., & Tang H. (2018). Spatiotemporal variations of hydrogeochemistry and its controlling factors in the Gandaki River Basin, Central Himalaya Nepal. *Science of the Total Environment*, **622**, 770-782.

Panthi J., Dahal P., Shrestha M., Aryal S., Krakauer N., Pradhanang,S., ... & Karki R. (2015). Spatial and temporal variability of rainfall in the Gandaki River Basin of Nepal Himalaya. *Climate*, **3(1)**, 210-226.

Quade J., English N., & DeCelles P. G. (2003). Silicate versus carbonate weathering in the Himalaya: a comparison of the Arun and Seti River watersheds. *Chemical Geology*, **202(3-4)**, 275-296.

Sarin M. M., & Krishnaswami S. (1984). Major ion chemistry of the Ganga–Brahmaputra river systems, India. *Nature*, **312(5994)**, 538.

Sarin M. M., Krishnaswami S., Dilli K., Somayajulu B. L. K., & Moore W. S. (1989). Major ion chemistry of the Ganga-Brahmaputra river system: Weathering processes and fluxes to the Bay of Bengal. *Geochimica et cosmochimica acta*, **53(5)**, 997-1009.

Sarmiento J. L., & Gruber, N. (2006). Ocean biogeochemical dynamics. Princeton University Press.

Sequeira R., & Kelkar D. (1978). Geochemical implications of summer monsoonal rainwater composition over India. *Journal of Applied Meteorology*, **17(9)**, 1390-1396.

Shrestha A. B., Wake C. P., Dibb J. E., & Whitlow S. I. (2002). Aerosol and precipitation chemistry at a remote Himalayan site in Nepal. *Aerosol Science and technology*, **36(4)**, 441-456.

Singh S. P., & Singh B. P. (2010). Geothermal evolution of the evaporite-bearing sequences of the Lesser Himalaya, India. *International Journal of Earth Sciences*, **99(1)**, 101-108.

Tipper E. T., Bickle M. J., Galy A., West A. J., Pomiès C., & Chapman H. J. (2006). The short term climatic sensitivity of carbonate and silicate weathering fluxes: insight from seasonal variations in river chemistry. *Geochimica et Cosmochimica Acta*, **70(11)**, 2737-2754.

Tripathee L., Kang S., Huang J., Sharma C. M., Sillanpää M., Guo J., & Paudyal R. (2014). Concentrations of trace elements in wet deposition over the central Himalayas, Nepal. *Atmospheric environment*, **95**, 231-238.

Torres M. A., Moosdorf N., Hartmann J., Adkins J. F., & West A. J. (2017). Glacial weathering, sulfide oxidation, and global carbon cycle feedbacks. *Proceedings of the National Academy of Sciences*, **114(33)**, 8716-8721.

Tshering L. D., & Bhandari A. N. (1973). Geological report on the Salt Occurrences of Mustang area. Ministry of Industry & Commerce, Nepal Geological Survey.

Turchyn A. V., Tipper E. T., Galy A., Lo J. K., & Bickle M. J. (2013). Isotope evidence for secondary sulfide precipitation along the Marsyandi River, Nepal, Himalayas. *Earth and Planetary Science Letters*, **374**, 36-46.

Valdiya K.S. (1980) Geology of the Kumaun Lesser Himalayas. Wadia Institute of the Himalayan Geology, Dehra Dun, India.

West A. J., Bickle M. J., Collins R., & Brasington J. (2002). Small-catchment perspective on Himalayan weathering fluxes. *Geology*, **30(4)**, 355-358.

Wolff-Boenisch D., Gabet E. J., Burbank D. W., Langner H., & Putkonen J. (2009). Spatial variations in chemical weathering and CO_2 consumption in Nepalese High Himalayan catchments during the monsoon season. *Geochimica et Cosmochimica Acta*, **73(11)**, 3148-3170.